Arabian Journal for Science and Engineering (2023) 48:497–514
https://doi.org/10.1007/s13369-022-07283-6

RESEARCH ARTICLE-CHEMISTRY

Novel Physically Cross-Linked Curcumin-Loaded PVA/Aloe vera Hydrogel Membranes for Acceleration of Topical Wound Healing: In Vitro and In Vivo Experiments

El-Refaie S. Kenawy[1] · Elbadawy A. Kamoun[2,3] · Zeinab S. Ghaly[1] · Abdel-baset M. Shokr[1] · Mahmoud A. El-Meligy[1] · Yehia A.-G. Mahmoud[4]

Received: 12 March 2022 / Accepted: 8 September 2022 / Published online: 26 September 2022
© The Author(s) 2022

Abstract

This study aims to prepare novel cross-linked antimicrobial membranes composed of PVA-Aloe vera hydrogels using novel physically cross-linked method via transforming PVA to high crystalline structure using propanol. Curcumin was incorporated to improve the membrane biological properties; while gentamycin improved sharply antimicrobial properties. PVA-Aloe vera hydrogel membranes were analyzed by FTIR, SEM, XRD and TGA measurements for characterizing resultant cross-linked membranes. Physicochemical measurements, e.g., swelling and mechanical stability were assessed for further studying the dressings. Antibacterial activity of cross-linked PVA-Aloe vera-curcumin membranes was tested using five bacterial strains. Results showed that high Aloe vera content in cross-linked membranes has insignificant impact on the release of gentamicin. Adult *Wister Albino* rats were used to test membrane's ability for improving the wound healing rate in vivo. In vivo findings showed that PVA/Aloe vera/curcumin membranes dramatically reduced the size of mouse full-thickness wounds, as indicated by a decrease in the wound size. Furthermore, histological tests of wounds dressed with membranes revealed a significant re-epithelialization; compared to wounds treated with cotton gauze and PVA/Aloe vera dressings without curcumin, showing curcumin's efficacy. These results refer to PVA-Aloe vera-curcumin membrane has exceptional wound healing and skin regeneration capacity.

Keywords PVA-Aloe vera hydrogel membranes · Physical cross-linking · Curcumin · In vitro and in vivo study

1 Introduction

Healing of wound is a reaction to injured tissue leading to the restoration of tissue integrity. Hydrogels are a clear gel at body temperature, fill the wound spaces and protect the wound area from bacterial infection. Thus, hydrogels were well employed as wound dressing materials with high flexibility, mechanical stability, and good penetrability to water vapor and metabolites, which entirely protect the wound [1]. Basically, hydrogels absorb and retain famous wound exudates, which stimulate fibroblast proliferation and keratinocyte migration. The last two processes are very essential for continuing the epithelialization and accelerating healing rate of the wound [2]. As well, the compacted mesh size of hydrogels structure hinders the wound core from any bacterial invasion. However, hydrogels can easily transfer the bioactive molecules, e.g., antibiotics and pharmaceuticals to wound zone [3]. Poly (vinyl alcohol) (PVA) stands out among synthetic polymers because of its excellent biocompatibility

✉ El-Refaie S. Kenawy
ekenawy@yahoo.com

✉ Elbadawy A. Kamoun
e-b.kamoun@tu-bs.de,badawykamoun@yahoo.com

[1] Polymer Research Group, Department of Chemistry, Faculty of Science, University of Tanta, Tanta 31527, Egypt

[2] Nanotechnology Research Center (NTRC), The British University in Egypt (BUE), El-Sherouk City, Cairo 11837, Egypt

[3] Polymeric Materials Research Dep, Advanced Technology and New Materials Research Institute (ATNMRI), City of Scientific Research and Technological Applications (SRTA-City), New Borg Al-Arab City, Alexandria 21934, Egypt

[4] Botany Department, Faculty of Science, Tanta University, Tanta 31527, Egypt

and protection [4, 5]. PVA was well known as the proper candidate that was used for releasing biological and medical matters in a sustained release behavior [6]. In addition, PVA possesses exclusive properties, such as chemical resistance, average thermal stability, and high biocompatible/nontoxic biomaterial [7]. Also, PVA was studied intensively, owing to its easy film-forming and feature physicochemical properties [7]. Meanwhile, PVA has been chemically cross-linked with several chemical cross-linkers including glutaraldehyde, acetyl aldehyde, or formaldehyde [8, 9]. Herein, we sought to escape from using traditional chemical cross-linkers in order to mitigate the introduction of reactive species, that could somewhat restrict the biocompatibility of prepared membranes. Methods were known that produce physically cross-linked hydrogels of PVA via the partial crystallization, in particular, the alternate freeze-thawing technique applied to PVA solutions [10]. However, an apparently new and simple entanglement method to physically cross-linked PVA was reported to obtain 100% hydrolyzed PVA fibers using lower alcohols such as methanol, instead of traditional chemical cross-linking [11].

Aloe vera was recognized as the oldest therapeutic herb, and it could easily accelerate the rate of wound healing and treat burned area on the optical skin. *Aloe vera* consists of two main ingredients: one in the outer layer is vascular bundle and in the other in the inner layer is colorless *parenchyma* containing *Aloe vera* gel. *Aloe vera* contains three compositions that embrace structural, chemical and polysaccharides; where polysaccharides play the key role in enhancing the wound healing ability. Polysaccharides contain salicylic acid together with other complexes such as proteins, lipids, amino acids, vitamins, enzymes, inorganic compounds and small organic compounds [12–14]. Acemannan is a kind of active polysaccharide present in *Aloe vera* that strongly inhibits the bacterial growth and stimulate macrophage activity [15]. Moreover, the anti-inflammatory and antioxidant properties of *Aloe vera* were previously discussed and investigated [16, 17]. Thus, *Aloe vera* was chosen as a typical model for accelerating the rate of wound healing process.

A number of assumptions were proposed for the effect of *Aloe vera* gel on wound healing parameters, which include keeping the wound moist, increase epithelial cell migration, more rapid maturation of collagen and reduction in inflammation [12]. Curcumin is a polyphenol resultant from the turmeric (*Curcima longa*) roots. Curcumin was studied intensively in particular as very active ingredient due to its anti-inflammatory, antioxidant, and anti-proliferative properties. Many research works have reported that curcumin usage has a very quick action by increasing collagen, fibroblast, and vascular density during wound healing. Also, curcumin acts as a proangiogenic agent in healing process by initiating transforming growth factor beta ($TGF\text{-}\beta$) [18, 19], whereas similar studies exposed the optimistic responses toward wound healing in different regions of body with targeted curcumin application [18, 20–25].

In this research, we developed novel physically cross-linked curcumin-loaded PVA/Aloe vera hydrogel membranes using traces of propanol for fully hydrolyzed PVA, avoiding the toxicity of traditional chemical cross-linkers. Physicochemical properties and its characterization of obtained hydrogel membranes were measured and discussed in detail. In addition, bioevaluation tests both in vitro and in vivo of obtained cross-linked PVA/Aloe vera hydrogel membranes were assessed in detail, particularly in terms of ability of tested biomaterials for accelerating the wound healing.

2 Materials and Methods

2.1 Materials

Polyvinyl alcohol (PVA, Mwt. 75 KD, 99.0% hydrolysis) was obtained from Sigma-Aldrich, Germany. Aloe vera gel was freshly extracted from local garden from Tanta, Egypt. Curcumin (Mwt. 368.38) was gotten from BIO-BASIC INC., Canada. Propanol (purity 99.0%) was obtained from Alfa-Aesar China Limited. RPMI-1640 medium, MTT and DMSO were purchased from (Sigma-Aldrich, St. Louis, USA). Fetal bovine serum (FBS) was obtained from (GIBCO, UK). Doxorubicin was obtained from (Sigma-Aldrich, Germany) that was used as a standard anticancer drug. Human lung fibroblast cell line (WI38) and mouse connective tissue fibroblast cell line (L929) were commercially obtained from ATCC via Holding Co. for Biological Products and Vaccines (VACSERA), Cairo, Egypt.

2.2 Extraction of Aloe vera Gel from Leaves

Aloe vera leaves were gathered from a local garden located in Tanta City, Gharbeya, Egypt, where *Aloe vera* leaves were collected freshly on the same day of experiment. *Aloe vera* leaves mean diameters were between 30 and 50 cm long when freshly picked, indicating its three-year-old plant. To extract and purify soil from leaves, the leaves were washed in distilled water carefully at room temperature. Then, leaves were clipped transversely into pieces after spikes along the margin were removed, and the dense epidermis was carefully separated from the parenchyma by a sharp blade, as described elsewhere [26, 27]. Before being homogenized in a blender, the parenchyma was thoroughly washed gently again with distilled water at ambient conditions to extract surface exudates. To extract fibers, the homogenized gel was centrifuged at 3000 rpm for 30 min. The supernatant was obtained by vacuum-filtered over a filter paper (Whatman, Germany) to get fresh *Aloe vera* gel. The obtained Aloe vera

Table 1 Sample codes and membranes composition for different curcumin-/gentamicin-loaded PVA/Aloe vera/curcumin cross-linked membranes

Composition of samples	10 (wt%) PVA content (ml)	*Aloe vera* content (ml)
100% PVA/0% Aloe vera	25	0
80% PVA/20% Aloe vera	20	5
60% PVA/40% Aloe vera	15	10
40% PVA/60% Aloe vera	10	15
20% PVA/80% Aloe vera	20	5

gel was directly used and incorporated into hydrogel preparation to avoid its color change.

2.3 Preparation of Physically Cross-linked Curcumin-Loaded PVA/Aloe vera Hydrogel Membranes

10 (wt.%) of PVA is dissolved in distilled water at ambient conditions, and then *Aloe vera* extract was mixed to PVA solution in different ratios and coded as shown in Table 1, where PVA/*Aloe vera* mixture solution was kept under stirring at 50 °C for 2 h. Then, curcumin solution is added to the PVA/*Aloe vera* mixtures to reach final concentration 20 μg/ml; furthermore, gentamicin was added in concentration of 1.5 mg/ml to PVA/Aloe vera solution at room temperature, using traditional casting-solution method in *petri* dishes (9 cm diameter). Curcumin-loaded PVA/Aloe vera/gentamicin physical cross-linked hydrogel membranes is obtained and formed after membranes were soaked in propyl alcohol for 6 h [28].

2.4 Characterization of Hydrogel Membranes

Curcumin-loaded PVA/Aloe vera/gentamicin hydrogel membranes were instrumentally characterized to verify the entanglement reaction via chemical structure analysis by FTIR-ATR and XRD. While surface morphological investigation, thermal and mechanical stability of hydrogel membranes were analyzed by SEM, TGA and universal tensile testing machine; respectively. The sample preparation and each measurement or analysis were discussed in details in (supplementary information).

Physicochemical Measurements of Curcumin-Loaded PVA/Aloe vera Hydrogel Membranes.

Physicochemical properties of obtained hydrogel membranes, e.g., gel fraction (GF%), swelling ratio (%), wettability index and in vitro release profile were studied and discussed, where all measurements procedures were adapted from our previous published research works (supplementary information) [28–31].

2.5 Bioevaluation Tests

2.5.1 In Vitro Assessments

Hemocompatibility Assay Hemolysis experiment was performed topically on the obtained curcumin-loaded PVA/Aloe vera membranes, as previously studied [32, 33]. Membranes were soaked in saline solution (NaCl, 0.9 w/v at 37 °C for 24 h). In this test, anti-coagulated blood is required, which was obtained by mixing one ml of anti-coagulated acid citrate dextrose solution (ACD) with 9 ml of fresh human blood from adult donor (male with 30 years old, 86 kg). The equilibrated curcumin-loaded PVA/Aloe vera hydrogel films (8 cm^2) were moved into PP test tubes and incubated for 72 h with 7 ml of phosphate buffer saline (PBS, pH 7.4). The PBS in the last test tubes was removed, and 1 ml of ACD solution was applied to each sample, which was then incubated for 3 h at 37 °C. The positive and negative controls were made by mixing the same volume of ACD with 7 mL of distilled water and PBS. The tube was incubated and gently inverted twice every 30 min to ensure that hydrogel films and ACD blood were in constant contact. The fluids were then moved to a proper tube and centrifuged again for 20 min at 3000 rpm. Calculation of hemoglobin is produced by hemolysis using optical densities (OD) of the supernatant. The absorbance of supernatant was monitored at 540 nm using aby spectrophotometer (Ultrospec 2000, Germany). The hemolysis (%) was determined by the given formula as follows:

$$\text{Haemolysis}\,(\%) = \frac{\left(\text{A ODsample} - \text{A ODnegative control}\right)}{\left(\text{A ODpositive control} - \text{A ODnegative control}\right)} \times 100. \quad (1)$$

where A is spectrophotometric absorbance value. A (sample of membrane) is absorbance value of tested membrane, *A*(− ve) control is absorbance of tube without membrane sample, which contains ACD solution and 7 ml PBS, and *A*(+ ve) control is absorbance of tube without membrane sample which contains ACD solution and 7 ml distilled water.

Antibacterial Activity Assay

- *Agar Diffusion Method*

The antimicrobial of tested membranes was tested by disk-diffusion method, as previously described elsewhere [34]. The sterile nutrient agar plates were prepared, where the bacterial test organisms, e.g., *Staphylococcus aureus, Klebsiella pneumonia, Escherichia coli and Acinetobacter* were extended over the nutrient agar plates by single sterile cotton buds. After the microbial lawn preparation, five unlike ratios of films disk were placed on the organisms. All bacterial plates were incubated at 37 °C for 24 h. The inhibition zone was measured in millimeter, while each sample was seeded and carried out triplicated for calculating the average.

- *Broth Spectrophotometric Method*

Bioassay methods, e.g., broth or agar dilution, well-diffusion and disk-diffusion were utilized for antibacterial mode screening [35]. Here, antibacterial activity of curcumin-loaded PVA/*Aloe vera*/gentamicin membranes was measured as previously discussed and reported [36]. Typically, the refreshed bacteria suspensions were diluted up to 100 times with 1% LB broth medium.100 μL of diluted suspension was cultured in a 10 mL of tryptone medium containing 0.1 g of tested sample, followed by sterilization at 120 °C for 20 min. Thereafter, the mixture was left under shaking for 18 h at 37 °C, and the growth inhibition percentage of bacteria was detected by estimation of the absorbance of the culture medium at 600 nm using visible spectroscopy. The inhibition (%) is calculated by the following equation:

$$\text{Inhibition}(\%) = [(A_a - A_b)/A_a] \times 100. \quad (2)$$

where A_b and A_a are the absorbance of bacterial culture in absence and in presence of tested sample, respectively.

Biodegradability Test Curcumin- and gentamicin-loaded cross-linked PVA/Aloe vera membranes were dried under vacuum-oven at 40°C for 24 h. Weighted (15 × 8 mm) dried membrane samples were soaked in 3 ml PBS (0.1 M). The samples were taken at predetermined intervals and then gently dried with soft tissue paper. The samples were then re-dried under the same drying conditions as before and then weighed. All of the experiments were carried out twice [29].

- *Cytotoxicity Test by MTT Assay*

Two different cell lines WI38 and L929 were cultured to determine the inhibitory effects of tested materials on cell growth by MTT assay [37, 38]. Cells were cultured in RPMI-1640 medium with 10% fetal bovine serum. Antibiotics were added with 100 unit/ml of penicillin and 100 μg/ml of streptomycin at 37°C in a 5% CO_2 incubator. Cells were seeded in a 96-well plate at a density of 1.0×10^4 cells/well at 37 °C for 48 h under 5% CO_2. After incubation, the cells were treated with tested membranes and incubated for 24 h. After 24 h of drug treatment, 20 μl of MTT solution at 5 mg/ml was added and incubated for further 4 h. 100 μl of DMSO is added into each well to dissolve the purple formazan formed. The colorimetric assay is measured and recorded at absorbance of 570 nm using a plate-reader (EXL 800, USA). The relative cell viability in percentage is calculated as given equation:

$$\text{Cell viability}(\%) = \left(A_{\text{treated samples}}/A_{\text{untreated sample}}\right) \times 100. \quad (3)$$

2.5.2 In Vivo Assessments

All in vivo tests were performed considering institutional ethical protocols approved by (Tanta University research committee, Egypt). These guidelines comprise appropriate methods for feeding, locating, and sacrificing rats in the in vivo experiments. In each group, rats number was initially equal to $n = 5$.

Wound Closure (%) Measurement All animal experiments were done based on "Guide for the care and use of laboratory animals." Male *Wister Albino* rats (8 weeks old, 200–250 g) were selected as animal model for testing wound healing parameters in vivo. After anesthetizing the rats via injection of xylazine (5 mg/kg body weight) and ketamine hydrochloride (100 mg/kg body weight), their dorsal hair was shaved gently. After the wound area was pre-prepared, *Wister* rats were randomly divided into four groups. Rats in the first group were treated with sterilized cross-linked PVA/Aloe vera hydrogel membranes, which were chosen based on in vitro results, while rats in the second group were treated with cross-linked curcumin-loaded PVA/Aloe vera hydrogel membranes. Similarly, rats in the third group were treated with cross-linked curcumin-loaded PVA/Aloe vera/gentamicin hydrogel membranes. Lastly, wounds of the fourth group were protected with a sterile layer of cotton gauze, as the negative control (NC).

All applied treatments were fixed with sterile gauze and medical fixation tape. While all scaffolds and the control dressings were replaced by new ones on the day of 3rd, 7th, 10th and 14th operation [39, 40], likely dressings were removed to assess wounds and analyze the percentage of wound closure. The wound reduction percentage is calculated using the given equation [39].

$$\%\text{wound contraction} = 1 - \frac{\text{wound area at the given day}}{\text{wound area at day zero}} \times 100. \quad (4)$$

Histological Study Skin tissues with wound sites were excised and immediately fixed in 10% neutral buffered formalin (pH ~ 7.2) for 48 h. After embed in paraffin and biopsies were sectioned to a 5 μm thickness, where sections were stained with hematoxylin–eosin (H&E). In histomorphometric study, epithelialization, inflammation, granulation tissue forming and collagen deposition were evaluated in different comparative groups. Also, these criteria were bioevaluated via semi-quantitatively on 5-point scale as follows: 0 (absent), 1 (25%), 2 (50%), 3 (75%), and 4 (100%). Results were validated by a comparative analysis of one-independent observer blinded to the treatment groups.

2.5.3 Statistical Analysis

Digital histological analysis, stained slides were scanned at 209 magnification using an *Aperio CS* bright field scanner (Leica Biosystems). Digital slides were then analyzed by *Image Scope program* (Aperio, Leica Biosystems). All scores were compared by *Kruskal–Wallis* analysis followed by *Dunn's test* to compare all means. Statistical analysis was accomplished using Prism (*GraphPad software*).

3 Results and discussion

3.1 Preparation of PVA Hydrogel Membranes

Herein, we sought to avoid the chemical cross-linking method of PVA, so as to aid and mitigate the addition of reactive species that could comprise biocompatibility. Physically cross-linked PVA over partial crystallization, particularly the alternative freeze-thawing technique, was offered previously [28]. However, a new and simple treatment to physically cross-linked electrospun PVA nanofibers using lower alcohols; such as methanol that preserves the integrity of the nano-mate as was reported by Yao et al. [11]. In the current work, it was proposed a new cross-linked PVA hydrogel membrane via traditional casting-solution method for fully hydrolyzing PVA, using low amounts of propanol which forms arranged/uniform morphological cross-linked membrane (Fig. S1, Supplementary materials) and Scheme 1. The proposed reaction mechanism that explains the fully hydrolyzing of PVA by addition of alcohol has been previously stated [41, 42].

H–H bonds between water molecules and hydrogen bonds in PVA molecules were fragmented after addition of propanol; while new hydrogen bonds are formed between water and propanol molecules (Scheme 1). However, free energy when new hydrogen bonds form is almost compensating for needed energy to fragment the original interactions. Also, the system disorder increases with increasing entropy. Thus, the hydrocarbon chains are enforced between water molecules and breaking hydrogen bonds among water molecules, whereas -OH ends of propanol molecules can form new hydrogen bonds with water molecules; however, the hydrocarbon "tail" does not form hydrogen bonds. This implies that several original hydrogen bonds being broken are never substituted by new ones [41].

Figure S1 represents a photograph of the formed fully hydrolyzed PVA films that were formed after casting in petri dishes then drying for 24 h at 36 °C, followed by soaking in propanol for 8 h, the films show increasing in mechanical strength as propanol-treated membranes which aids to increase the crystallinity degree and hence the cross-linking degree of PVA films increases. This might happen by elimination of residual water inside hydrogel membrane meshes by propanol permitting PVA-water hydrogen bonding to be substituted by H–H bonding intermolecular PVA. This is resulting in additional crystallization, which was further evidenced previously by Yao et al. [11].

3.2 Physicochemical Characterization of Hydrogel Membranes

- *Gel Fraction (%)*

Figure 2 represents the gel fraction of cross-linked PVA-/Aloe vera-incorporated curcumin and gentamicin membranes. It is clear that the highest PVA content in membranes showed the highest obtained gel fraction (%) values due to the highest cross-linking degree occurring (Fig. 1a). However, incorporation of Aloe vera in high contents in membranes decreased gel fraction significantly which verifies that the PVA is cross-linked after soaking in propanol. This is owing to increasing the content of fully hydrolyzed PVA in membranes allowing forming more hydrogen bonding to be replaced by additional crystallization resulting in more stabilization and higher gel fraction forming of the membrane [11].

- *Swelling Ratio (%)*

Figure 2b presents the water uptake of curcumin- and gentamicin-loaded PVA/Aloe vera cross-linked membranes. As seen, PVA hydrogel membrane containing curcumin and gentamicin displayed the least water uptake, while incorporation of Aloe vera into PVA/curcumin/gentamicin membranes increases dramatically the swelling degree. Notably, increasing the content of Aloe vera strongly increases the water absorbability of prepared membranes, and this might be due to the highly hydrophilic nature of Aloe vera and increases randomly the distribution of amorphous pours Aloe vera gels in the arranged crystalized PVA hydrogel membranes [11].

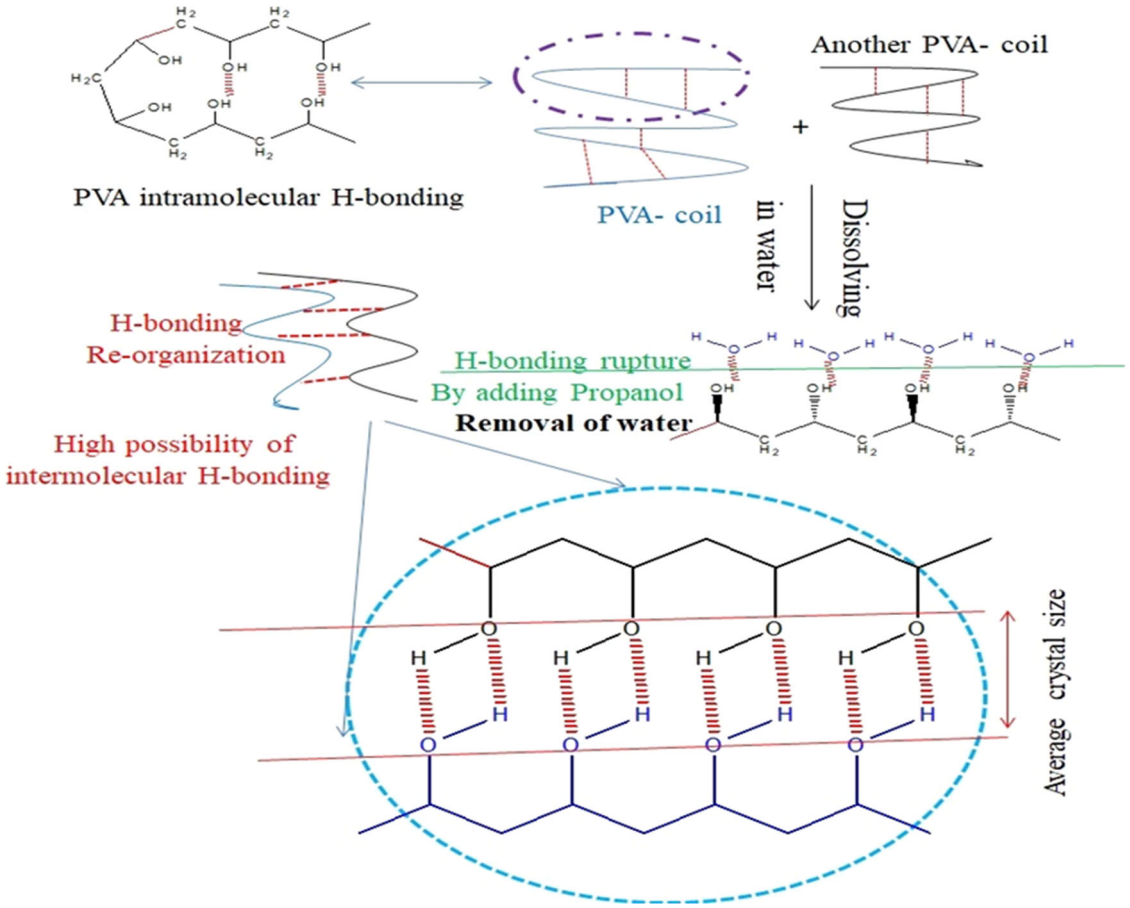

Scheme 1 Proposed reaction mechanism representing physically cross-linked and fully hydrolyzing PVA hydrogel membranes via propanol addition

- *Wettability Index (Contact Angel Results)*

Curcumin-/gentamicin-loaded PVA hydrogel membranes showed the highest contact angel value ranged to 78.2°, which dramatically decreased to reach 27.7° with incorporating the Aloe vera to 80% in hydrogel membranes (Fig. 1c). The results of wettability index through contact angel test (Fig. 1c, and Fig. S2, Supplementary materials) are consistent with swelling measurements in Fig. 1a, where the hydrophilicity of hydrogel membranes increased markedly with high contents of Aloe vera in the formed membranes and decreasing PVA crystallized via hydrogen bonding through using propanol alcohol [11].

3.3 Instrumental Characterization of Hydrogel Membranes

- *FTIR Analysis*

Figure 2a displays IR spectra of native PVA, uncross-linked PVA membrane, entangled PVA membrane treated with propanol and PVA/Aloe vera membrane treated with propanol. Also, Fig. S2a (*Supplementary data*) shows IR spectra of uncross-linked PVA, cross-linked PVA, and cross-linked PVA/Aloe vera membranes. For native PVA and uncross-linked PVA membrane; the band at ν 3253 cm^{-1} is pointed to –OH stretching peak; while the peak at ν 1425 cm^{-1} is allocated to -OH groups [43]. Also, the vibrational band at ν 2925 cm^{-1} relates to asymmetric CH_2 group stretching peak. The peak at ν 1633–1561 cm^{-1} is attributed to C = C stretching vibration of PVA. Meanwhile, the peaks corresponding to C–O stretching occur at *ca.* ν 1081.4 cm^{-1}, while the band at ν 837.1 cm^{-1} is ascribed to C–C stretching vibration of PVA [44–46]. For cross-linked PVA/Aloe vera membranes; the typical –OH group bands of free unreacted alcohol (non-bonded –OH stretching band at ν 3650–3590 cm^{-1}) and hydrogen bonded bands (bonded –OH stretching bands at ν 3600–3200 cm^{-1}) are detected clearly. The hydrogen bonding between –OH groups can be detected among PVA chains, owing to formation of high hydrophilic forces [47].

- *XRD Analysis*

Figure 2b shows XRD patterns of native PVA, cross-linked PVA and PVA/Aloe vera cross-linked hydrogel membranes,

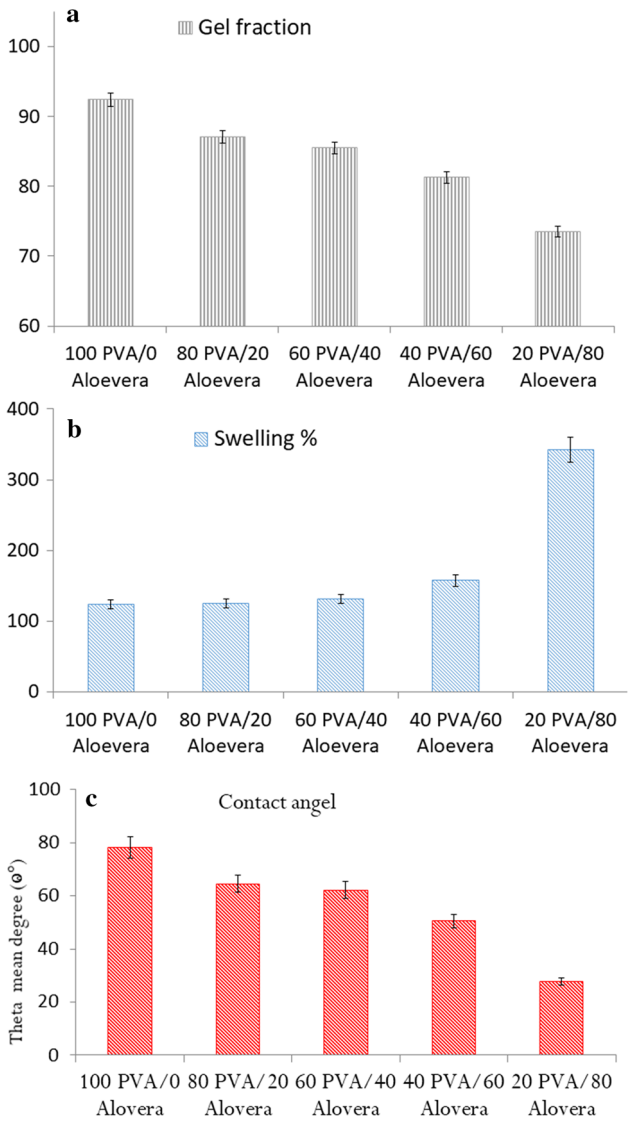

Fig. 1 Gel fraction (%) (**a**) and swelling ratio (%) (**b**) and wettability index via contact angel results (**c**) of PVA/Aloe vera hydrogel membranes incorporated curcumin and gentamicin cross-linked membranes

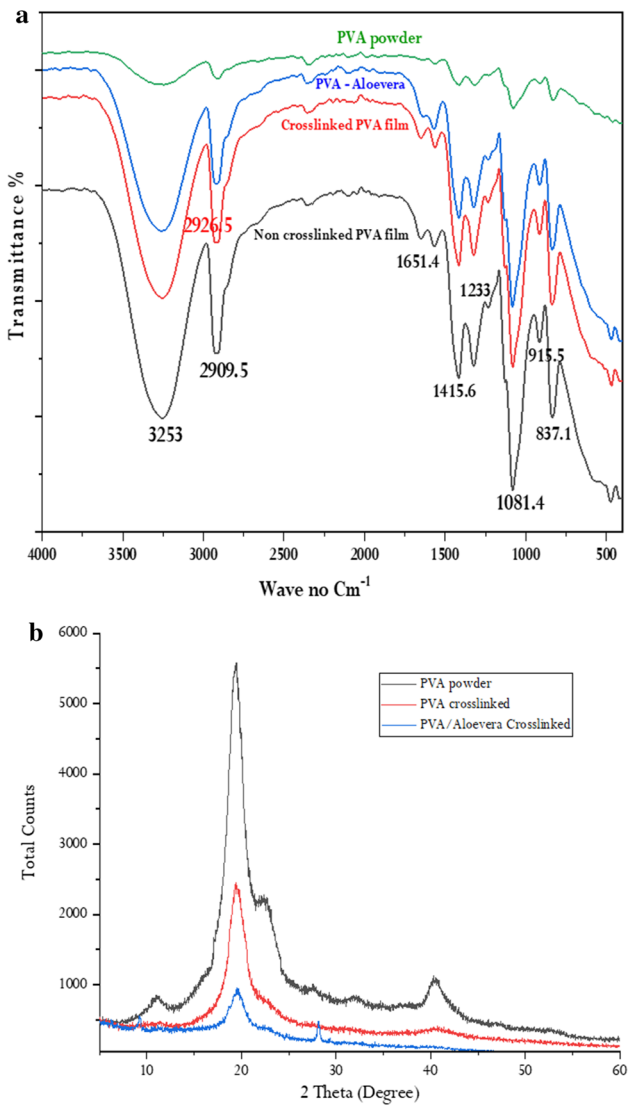

Fig. 2 ATR-FTIR spectra (**a**) and XRD patterns (**b**) of native PVA and PVA/Aloe vera hydrogel membranes with/without propanol treating

while Fig. S2b (*Supplementary data*) shows in detail separate XRD patterns of uncross-linked PVA, cross-linked PVA, and cross-linked PVA/Aloe vera membranes. All patterns showed the key diffraction peak of PVA at 2Θ ~ 18–19° [48]. This result is completely consistent with the hypothesis that non-cross-linked PVA was a partly crystalline substance which shows two peaks at 2Θ ~ 19.7° and 40.57° where the latter pattern sometimes overlaps with other patterns [42, 43]. While cross-linked PVA is a more crystalline than non-cross-linked which is presenting more peak area, the overlapped four patterns are detected at 2Θ ~ 19.7, 20.39, 23.6° and 41.24°. According to Scherer's equation [49], the total crystallization of entangled PVA by isopropanol increased by 77%, as the value of total crystallization of PVA non-cross-linked was found almost 0.93% that become 1.65% after treatment with isopropanol.

So, PVA crosslinking might be occurred physically via crystallization as the converting of intramolecular hydrogen bonding to be intermolecular hydrogen bonding increases the diffraction peaks. Notably, XRD results revealed that PVA and Aloe vera molecules in membranes were fully compatible, where PVA represents reflections from (d_{101}) a monoclinic unit cell, as shown by the strong crystalline reflection at 2Θ ~ 19.7 [50].

- *TGA Measurement*

TGA thermographs of various ratios of PVA-/Aloe vera-based stabilized hydrogel membranes formed containing

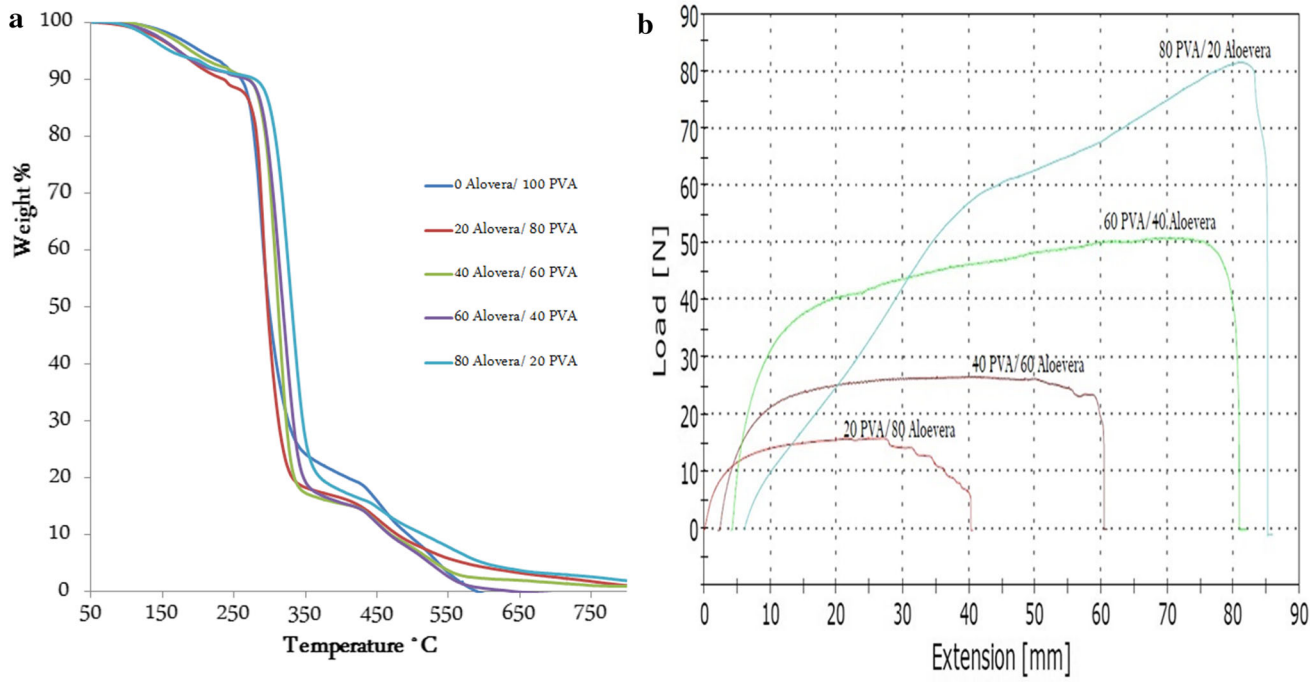

Fig. 3 TGA thermographs results (**a**) and mechanical measurements parameters (**b**) of curcumin-/gentamicin-loaded PVA/Aloe vera cross-linked membranes

Table 2 TGA results of curcumin-/gentamicin-loaded PVA/Aloe vera cross-linked membranes, the 25, 50 and 75% of weight loss (%) of initial weight of membranes were measured

PVA: Aloe vera ratio	T50	T25	T75
20 PVA/80 Aloe vera	329.5	312	351.5
40 PVA/60 Aloe vera	318.2	301	337.5
60 PVA/40 Aloe vera	310	297	325
80 PVA/20 Aloe vera	295.5	283.5	316.8
100 PVA/0 Aloe vera	298.5	281	343.5

curcumin and gentamicin are displayed in Fig. 3a, showing alterations in thermal decomposition behavior as mass loss percentages**.** The thermal decomposition temperatures at weigh loss 25, 50, and 75% of the initial weight of samples were expressed as (T_{25}, T_{50} and T_{75}), respectively, and briefly listed in Table 2.

The first thermal degradation stage at 50–150 °C could be assigned to the elimination of remained traces of humidity or solvent. The second thermal decomposition stage was monitored at 250–500 °C which results in the maximum residual weight loss %. This is owing to the thermal decomposition and volatilization of organic pieces of polymer. The third thermal decomposition stage was detected after approximately 550–800 °C, the whole thermographs turn into flat and most organic residues are completely volatilized forming ash. It is clear that, the temperature at which the membrane samples loss 50% increased with increasing the content of Aloe vera, as illustrated in Table 2, this indicates that addition of Aloe vera enhanced the thermal stability of PVA/Aloe vera membranes. This is because the hydroxyl groups of Aloe vera perhaps formed H–H bonding with those of PVA; and the higher thermal stability over native Aloe vera. Summarized TGA data in Table 2 are mostly consistent with the published data by Kenawy et al. [28], who offered that the adding of HES to PVA enriched thermal stability of PVA-HES hydrogel membranes.

- *Mechanical Properties*

Generally, an increase in the mechanical properties was mainly achieved by bonding the hydroxyl groups along PVA chains with propanol forming hydrogen bonds, where the resultant cross-linked PVA membranes are insoluble in common polar and nonpolar solvents. It was found that, increasing the crosslinking degree might depend on amount of PVA in membrane which is responsible for forming hydrogen bonds with propanol, resulting in increasing the applied force in mechanical strength measurement as listed in Table 3.

Table 3 illustrates the mechanical measurements parameters of fabricated cross-linked membranes with different ratios of PVA and Aloe vera. From Table 3 and Fig. 3b; it is obvious that there is a progressive increase in the applied force required for cutting the membranes, in addition to a

Table 3 Mechanical stability measurement parameters of curcumin-/gentamicin-loaded PVA/Aloe vera cross-linked membranes

PVA: Aloe vera ratio	Thickness (mm)	Force (N)	Tensile stress (MPa)	Extension (mm)
100 PVA/0 Aloe vera	0.39	157.01149	26.83957	135
80 PVA/20 Aloe vera	0.27	109.80336	24.3129	85
60 PVA/40 Aloe vera	0.19	81.54831	20.01624	76
40 PVA/60 Aloe vera	0.17	50.99785	15.46836	60
20 PVA/80 Aloe vera	0.13	26.80592	13.74663	40

clear increase in the extinction of membranes in case of increasing the PVA content. Unlike, a decrease in the content of Aloe vera resulted in a strong physically cross-linked formed network of PVA molecules via forming intermolecular hydrogen bonding.

- *SEM Investigation*

SEM micrographs in Fig. 4 present the surface and cross section morphological alternation due to differing the ratio of PVA: Aloe vera in cross-linked membranes, where the high Aloe vera content members showed more destroyed, amorphous and irregular surface of membranes, while cross section exhibited filamentous shape structure. However, the PVA content membranes exhibited arranged and regular surface shape structure and some vertical stacks tubes/channels-like shape in the cross section investigation mode, as shown in Fig. 4.

These observations are due to the high formed crystals resulting in intermolecular hydrogen bonding, forming tight and compressed structure [11]. However, the highest Aloe vera content membranes showed a porous surface structure, that serves to increase the hydrophilicity evidencing our results of contact angel and swelling ratio in Fig. 1.

- *Gentamicin Release Profile*

The calibration curve of gentamicin at 255 nm is represented in Fig. S4 (supplementary information). The cumulative released gentamicin from PVA/Aloe vera hydrogel membranes, as function of different ratios of (PVA: Aloe vera) in phosphate buffer (pH 7, at 37 °C), is shown in Fig. 5a. The initial release rate of gentamicin from PVA/Aloe vera hydrogels was rapid and ranged between 40 and 92%, mostly after the first 15 min of release profile. This initial "burst release" perhaps is owing to fast release or distribution of gentamicin, that was loaded closely to the surface-layer of membrane, and owing to the de-swelling of the gentamicin-loaded hydrogel in the buffer solution. However, it reaches to the leveling-off and maximum released gentamicin from 100 PVA/zero Aloe vera, 80 PVA/20 Aloe vera, 60 PVA/40 Aloe vera, 40 PVA/60 Aloe vera and 20 PVA/80 Aloe vera was obtained after 4 h, 3 h, 2 h, 30 min and 10 min, respectively. Furthermore, released gentamicin was markedly increased with increasing Aloe vera contents in PVA/Aloe vera membranes. These findings are consistent with previous results obtained by El-Lakany et al. [51], where they demonstrated that incorporation of additional amount of membranes composition beside zein protein nanofibers could increase the release profile of loaded α-Bisabolol drug. Similarly, the released ketoprofen from electrospun PVA mats significantly increased with the low concentrations of cross-linked PVA in nanofibrous mats [6].

The increase in released gentamicin as Aloe vera content rises could be recognized to the development of spongy and porous interior structure of PVA/Aloe vera hydrogels containing high Aloe vera contents, as was verified by SEM micrographs (Fig. 4). Moreover, high Aloe vera content in membranes facilitates the diffusion of loaded gentamicin, due to high water uptake probability as aforementioned verified in (Fig. 1b). This implies that the released gentamicin from PVA/Aloe vera membranes is regarded for most controlled-diffusion during high swellability and porous structure of carrier hydrogel membranes. The increase in crystallinity in the polymer consequently resulted in a decrease in diffusivity of PVA hydrogel and slowed down drug release rate [30, 39].

- *Hydrolytic Degradation*

Figure 5b shows the weight loss (%) of hydrogel membranes as function of time, where 100% PVA hydrogel membrane lost ~ 6–8% after 48 h. However, the weight loss (%) of PVA/Aloe vera hydrogel membranes dramatically increased to 10–27% after 48 h, with increasing Aloe vera content in membranes. This might be due to cross-linked PVA resulting from soaking in propanol that allows to form more hydrogen bonding which might be replaced by additional crystallization resulting in more stabilization and less biodegradable hydrogel membrane [11].

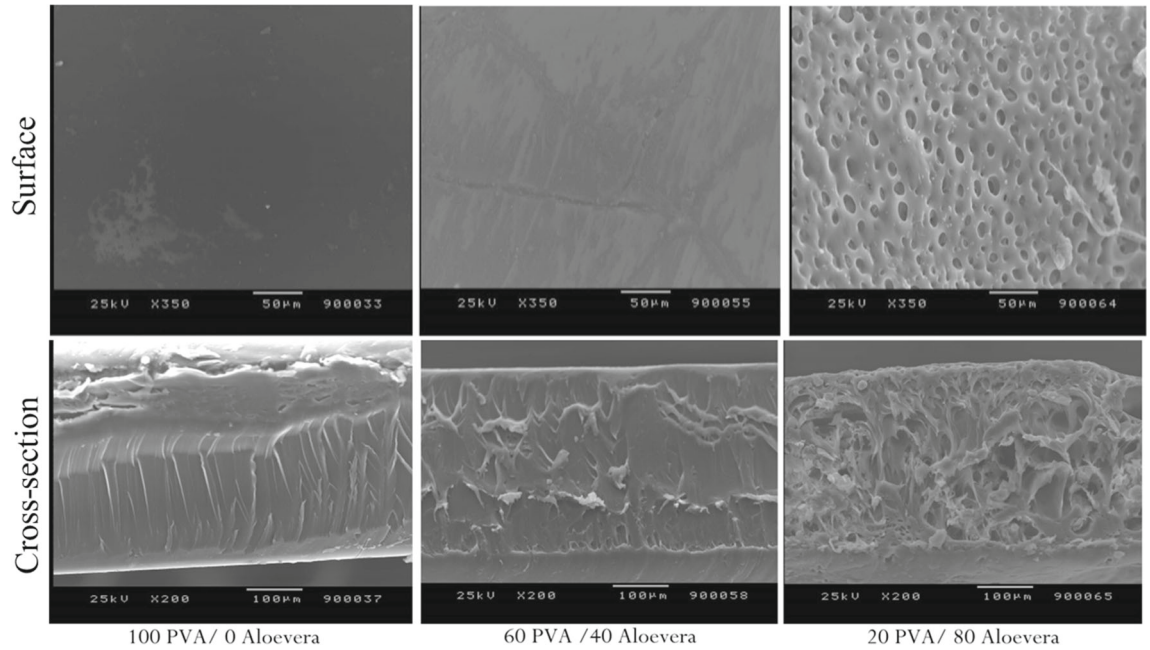

Fig. 4 SEM micrographs on the surface and cross section investigations of PVA and PVA/Aloe vera hydrogel membranes, (*surface*: original magnification × 350 and scale 50 µm) and (*cross section*: original magnification × 200 and scale 100 µm) at 25 kV

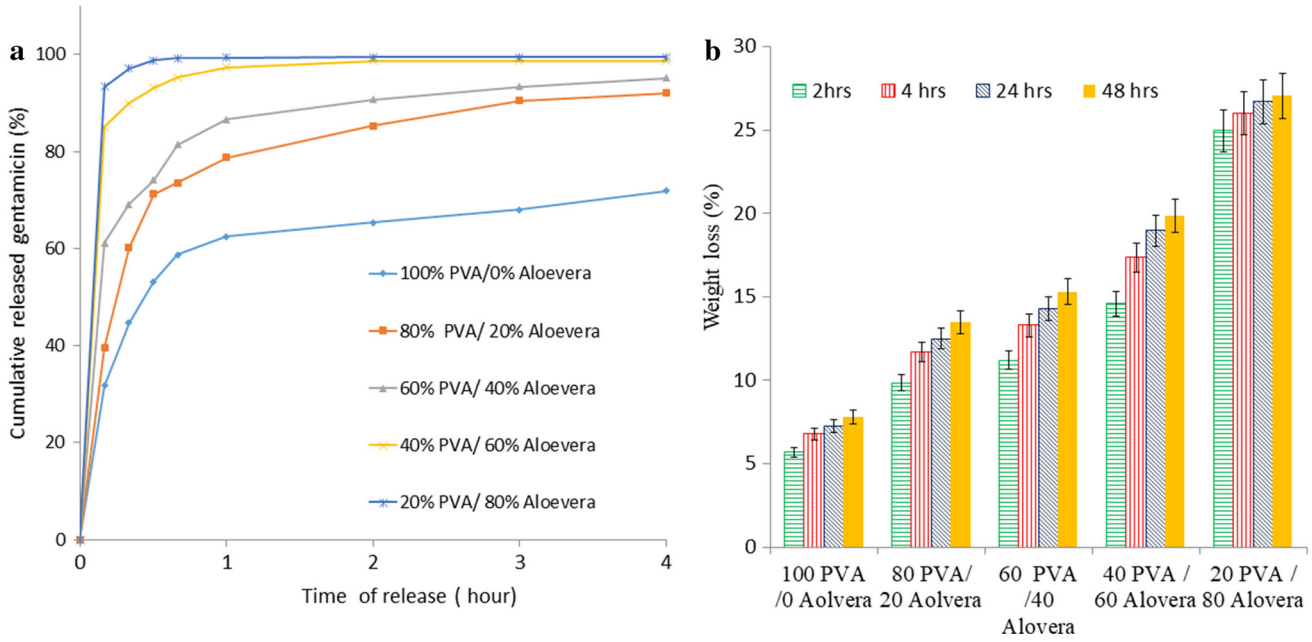

Fig. 5 Cumulative released gentamicin (%) from PVA and PVA/Aloe vera stabilized hydrogel membranes with different ratios of (PVA:Aloe vera) (**a**) and hydrolytic degradation profile of PVA/Aloe vera incorporated curcumin and gentamicin stabilized hydrogel membranes (**b**)

3.4 In Vitro Bioevalution Tests

3.4.1 Hemocompatibility

As seen, all tested samples of PVA/Aloe vera/curcumin hydrogel membrane possess accepted hemolytic values less than 2, that verifying all prepared membranes are non-hemolytic according to ASTM [29] and have good blood compatibility (Fig. 6). This attempt illustrates the blood tubes after centrifuged at 3000 rpm for 20 min containing positive and negative control tubes.

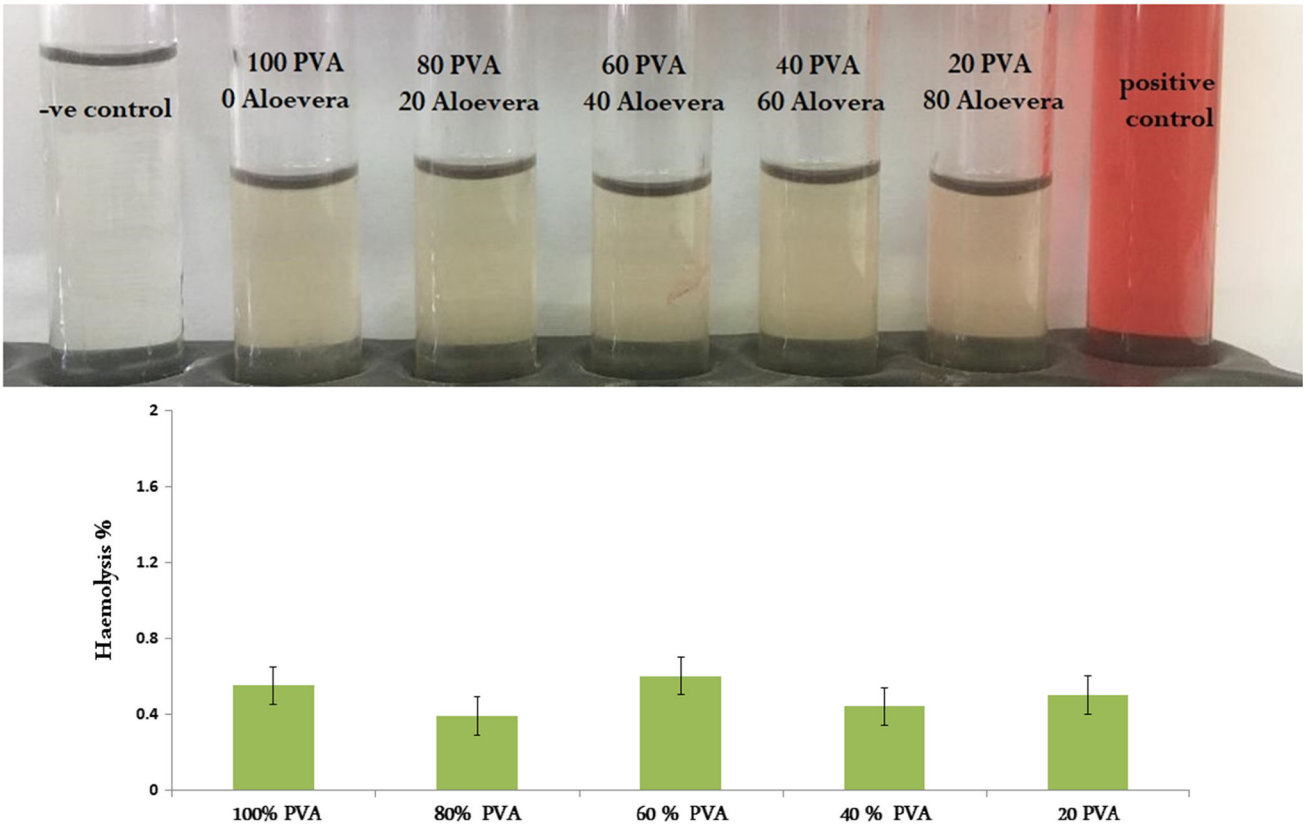

Fig. 6 Picture represents the blood tubes with blood compatible hydrogel membrane compositions (up) and hemolysis test results of tested PVA and PVA/Aloe vera hydrogel membranes (down)

3.4.2 Antibacterial Activity

PVA-/Aloe vera-incorporated curcumin hydrogel membranes showed slight effect of different constituent formed membranes against five different bacterial strains, three *Gram* negative (1S, *Klebsiella pneumonia*), (2S, *Pseudomonas aeruginosa*), (3S, *Escherichia coli*) and two *Gram* positive (4S, *staphylococcus aureus*) (5S *acinetobacter*) by agar disk-diffusion method using LB spectrophotometric method as represented in Fig. 7.

Therefore, this limitation of antibacterial activity of the prepared membranes derived us to support them with external antibiotics; such as gentamicin for improving their activity. However, the strong activity might prevent the wound infection virulence bacteria and accelerate the healing process during its application in vivo. Locally applied gentamicin is chosen for these reasons [52]: (1) It does not damage renal function; (2) limited risk of resistant pathogens and (3) killing bacteria by synthesis of inhibiting protein [53]. It can destabilize the lipid-bilayer membranes of bacteria [54, 55]. Systemically administered gentamicin might be toxic although, when locally managed even at very high concentrations, the serum concentrations are remaining well under toxic levels [56].

As presented in Fig. 7 and Table 4, gentamicin is effective against *Staphylococcus aureus* which is the most common bacterial infection in wounds and by using locally applied gentamicin. The defensive of in situ used gentamicin against wound infections in 'dirty and infected wounds' was previously reported [57].

Figure 7 and Table 4 represent the results of antibacterial activity of prepared membranes after loading the antibiotic. It is clear that the antibacterial inhibition percent increased from 74% for 50 PVA membranes to reach 96% for 10 PVA samples against *Klebsiella* strains, and from 89% for 50 PVA to 98% against *E-Coli* and increased from 93% for 50 PVA to 99% for 100% PVA against *Staphylococcus aureus* comparing with that of gram negative bacteria. Here, PVA was not previously reported as self-antibacterial effect, whereas curcumin offers a small antibacterial activity against a wide spectrum range that included both *Gram* negative and positive bacteria. These results are consistent with the reported results of Hussien et al. [58]; they reported that incorporation of curcumin into PVA/CNCs hydrogel membranes exhibited an antibacterial effect against wide spectrum of human pathogens of bacteria. The microbial inhibition of prepared samples might be owing to basically the effect of the antibiotic but the increasing effect, due to change in membrane

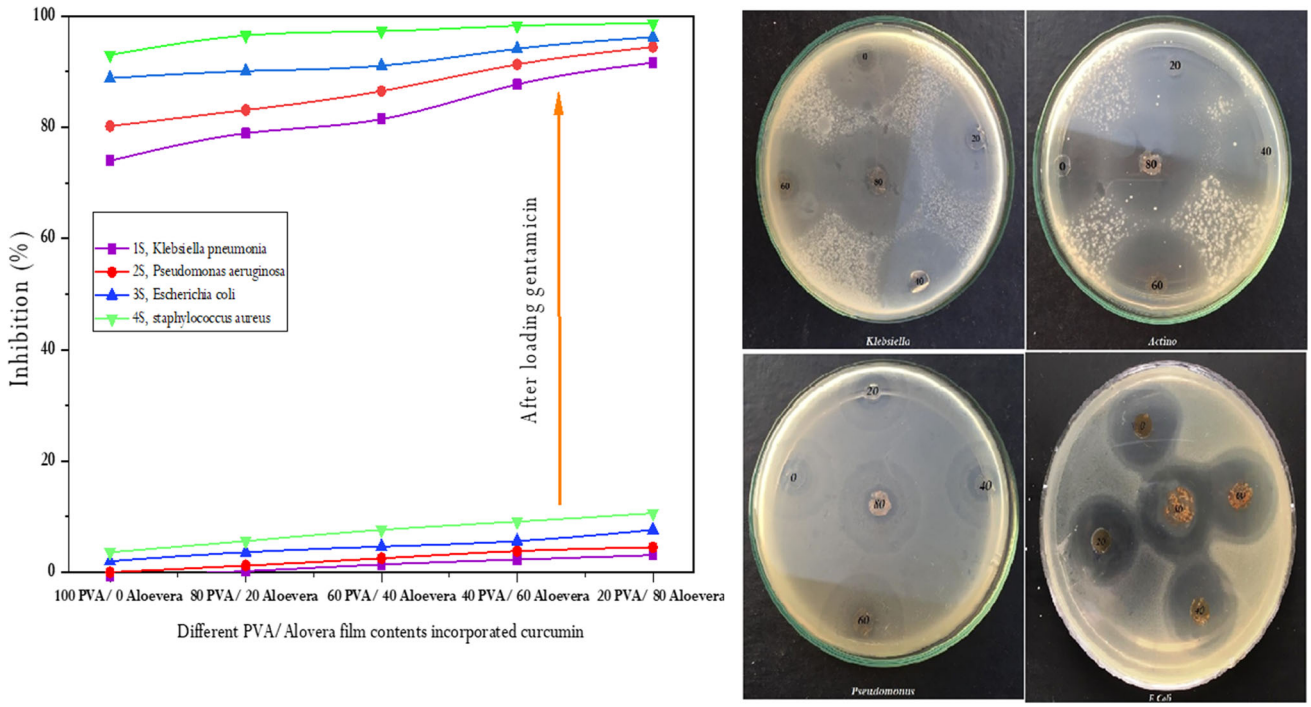

Fig. 7 Antimicrobial inhibition zone percent of PVA/Aloe vera cross-linked membranes incorporated curcumin and gentamicin (*left*). Pictures of antibacterial inhibition zone of PVA/Aloe vera incorporated gentamicin stabilized hydrogel membranes against four bacterial pathogens (*right*)

Table 4 Inhibition zone in (mm) of stabilized PVA/Aloe vera incorporated gentamicin hydrogel membranes against four bacterial pathogens

Hydrogel membranes (PVA: Aloevera)	Inhibition zone (mm)			
	Klebsiella	*E-Coli*	*Pseudomonas*	*Acintobacter*
20:80	20	18	12	18
40:60	18	17	11	17
60:40	17	15	10	16
80:20	15	13	9	14
100:0	14	11	8	12

composition resulting from increase in Aloe vera content from zero to 80% in the membranes. Furthermore, the cross-linking degree significantly reduced with the increase in the Aloe vera content in membranes; despite the cross-linking degree is mainly depending on the amount of PVA in membranes.

3.4.3 Cytotoxicity Test

Wound dressing candidate's cytotoxicity assay is a definitive method of determining if the materials under investigation should be further investigated in vitro and in vivo. Since the wound dressing agents will come into direct contact with *fibroblast*, *keratinocyte,* and *epithelial* cells through wound healing, thus this phase is critical [59]. Accordingly, in the presence of fabricated membranes, the cellular response was assessed using fibroblasts as pertinent cells at the wound bed, which are responsible for tissue granulation through the connective tissues regeneration accompanying with initiating the skin regeneration. The cytotoxicity of membranes was tested by MTT assay and showed nontoxic effect toward fibroblasts normal cell line.

Table 5 represents cytotoxicity results of PVA hydrogel membranes with different contents of Aloe vera incorporated curcumin. The results revealed that a significant decrease in cytotoxicity almost 51% for membrane contains 0% Aloe vera, that considered as a weak cytotoxic biomaterial [37, 38, 60] for *W138* cell line to reach more than 100% viable cells with the highest Aloe vera content. Furthermore, *L929* cell lines showed better cell viability with zero Aloe vera content that reached to 71% to be completely nontoxic with the highest Aloe vera content. This improvement of cell viability behavior might be due to the nature origin of Aloe vera.

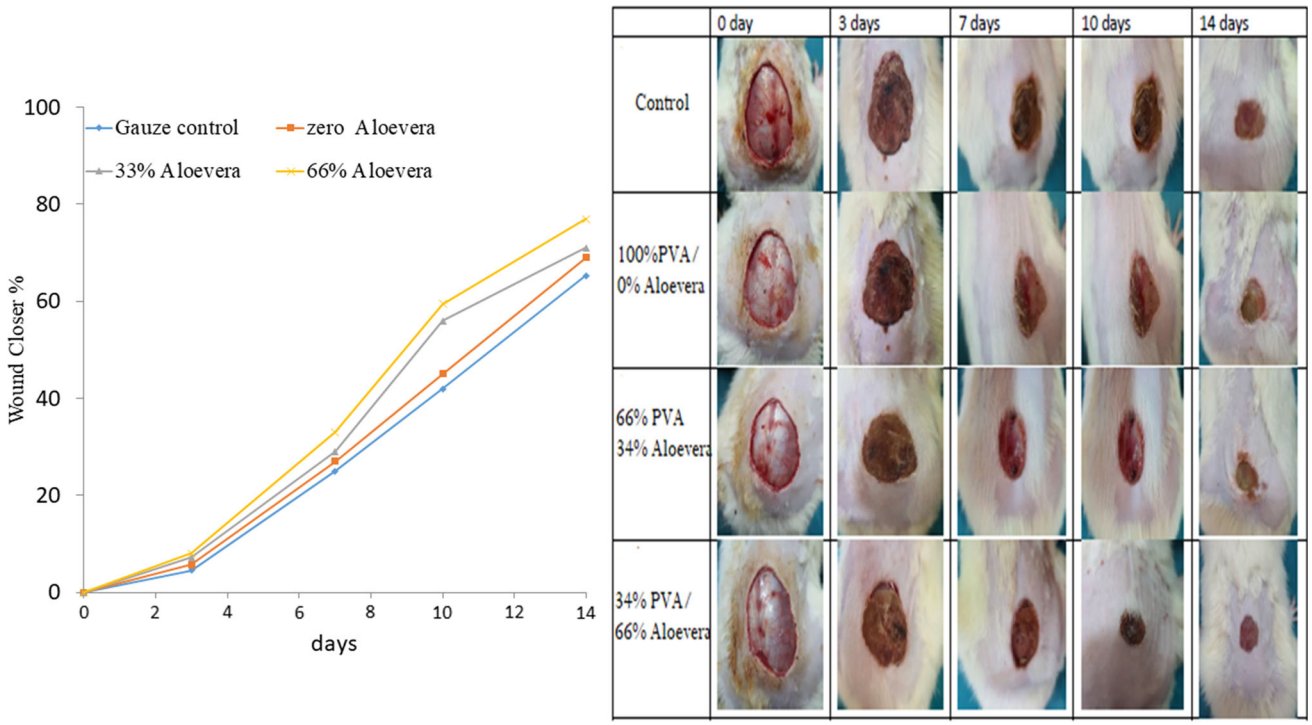

Fig. 8 Wound closure (%) of PVA/Aloe vera hydrogel membranes (*left*) and photographic image examination of the wounds size reduction and healing process after incorporation of Aloe vera with different ratios in membranes, after operation 0, 3, 7, 10, and 14 days (*right*)

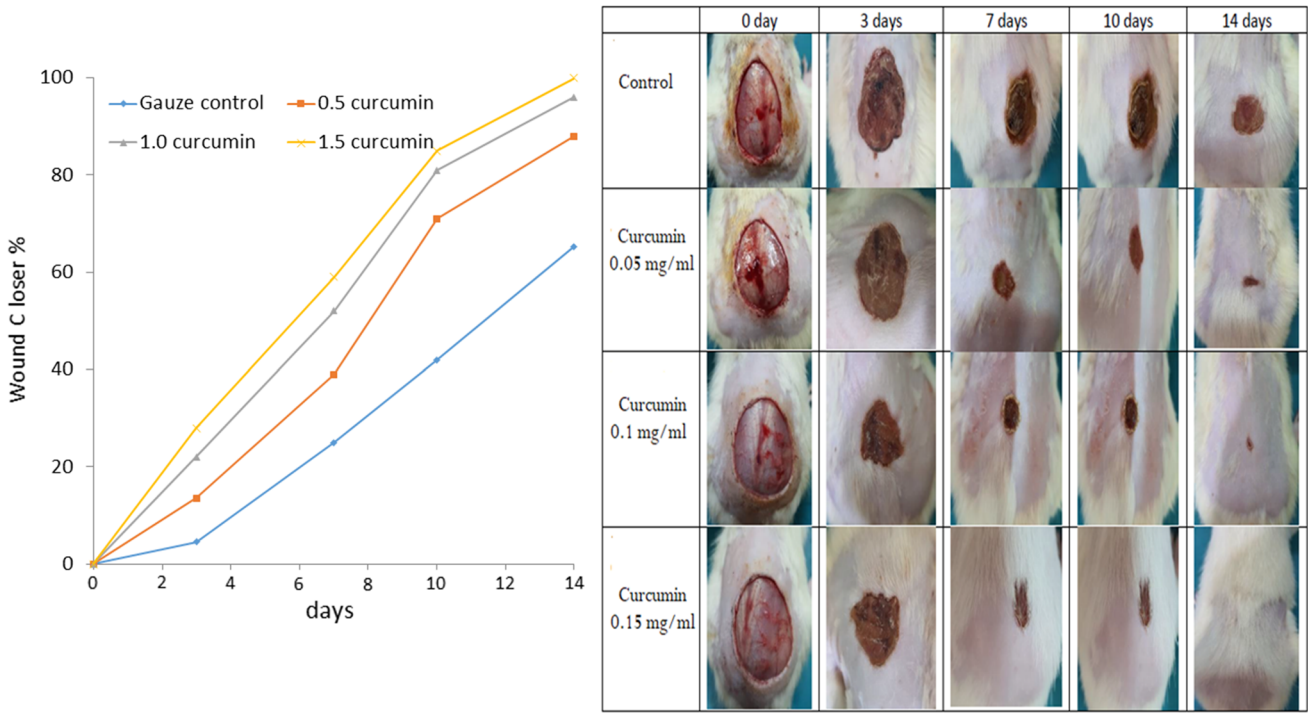

Fig. 9 Wound closure (%) of PVA/Aloe vera/curcumin hydrogel membranes (*left*) and photographic image examination of the wounds size reduction and healing process after incorporation of curcumin with different ratios in membranes, after operation 0, 3, 7, 10, and 14 days (*right*)

Table 5 Cytotoxicity results for PVA/Aloe vera/curcumin hydrogel membranes

No	Comp	In vitro cytotoxicity IC50 (μg)	
		WI38	*L929*
• •	DOX	6.72 ± 0.5	5.18 ± 0.2
1	10	100 <	100 <
2	20	91.26 ± 4.8	95.02 ± 3.7
3	30	79.05 ± 3.9	88.34 ± 3.3
4	40	65.14 ± 3.5	75.60 ± 3.0
5	50	51.39 ± 3.2	70.81 ± 2.8

IC50 (μg): 1–10 (very strong); 11–20 (strong); 21–50 (moderate); 51–100 (weak) and above 100 (non-cytotoxic)
DOX doxorubicin

3.5 In vivo Bioevalution Tests

3.5.1 Wound Closure (%)

The images of wound healing steps in the different groups on zero, 3rd, 7th, 10th and 14th days of in vivo attempts are displayed in Figs. 8 and 9 for wound diameter change monitoring with time. The observations of the wound closure (%) of the mentioned groups are presented in Figs. 8 and 9. As results, the wound size varied remarkably in all examined cases in 14th days of assessment ($P < 0.05$ for all of the samples, except for the NC group in 14th days of the treatment).

Recently, pharmaceutical application of Aloe vera plant is allocated into two parts: Aloe resins or Aloe anthraquinone which are existing in the outer layer of Aloe skin. Aloe resins consist of aloin, isobarbaloin and chrysaphanic barbaloine which are mostly semi-toxic compounds. The second part is Aloe gel, which is existing in the inner layer of the plant leaves and consisting of water with polysaccharides, acetylated glucomannan and other carbohydrates [61, 62]. While gel contains amino acids complex, salicylic acid, ascorbic acid, and vitamins A, E. Aloe leaves were found to activate the macrophage and adjust the cell immune system, fibroblasts, and granulocytes [63, 64]. In this study, Aloe leaves were used to extract the pure gel of Aloe vera which was prepared freshly and used immediately to avoid the oxidation and gel color change.

From Fig. 8, the healing effect was observed after 2 weeks in wounds treated with highest Aloe vera content of PVA/Aloe vera membranes exhibiting 75% wound closer. Compared to gauze, control group showed only about 65.5% wound closure. On day 7, all the prepared samples treated groups' wounds were partially healed with percent around 70%. Furthermore, gel experimental management was found to increase DNA and tissue power that stimulates formation of new vessels and epithelization [65, 66].

From Fig. 9, the noticeable healing effect was observed after 2 weeks in wounds treated with curcumin content membranes exhibiting more than 99% wound closer for highest curcumin content treated cases. Compared to gauze, the control groups showed only about 65.5% wound closure, compared to PVA/Aloe vera membranes free curcumin which offered almost 75% healing effect. The marvelous effect of curcumin has clear effects in all wound healing stages as the following:

- Inflammation Stage

Curcumin was employed as anti-inflammatory, anti-infectious, preventing the production of two cytokines (IL-1 and TNF-α) that initiate monocytes and macrophages which act in a vital role for handling the inflammatory response. Also, curcumin hinders the action of transcription factor of NF-(κ)B (nuclear factor kappa-light chain-improver of activated B cells), which controls the transcription of cytokines that regulate cellular differentiation, survival and proliferation. Also, NF-(κ)B contributes to development and survival of cells and tissues that carry out immune responses in mammals [67, 68]. Curcumin was exerted as antioxidant activity via scavenging action against ROS with low curcumin doses and increases ROS formation with high curcumin doses. Enhancing or reducing the production of antioxidant enzymes was found in dose-dependent manner [67].

- Proliferation Stage

Epithelialization or proliferation is the process in which keratinocytes transfer from the lower skin layers. Re-epithelialization, as a final phase of healing process, must be a robust process to return suitable wall function of the epidermis [62], and removing undesirable inflammatory cells from the wound-site.

- Remodeling Stage and Wound Contraction

Wound contraction is a part of the final stage of healing and comprises complex interactions among cells, extracellular matrix proteins and cytokines. Curcumin-treated wounds consistently showed a greater number of fibroblasts, which release positive *TGF-β* staining an important cytokine in the repaired tissues, chemo taxis, and collagen formation in the wound core [22].

3.5.2 Histological/Histomorphometric Analysis

Figure 10 shows microscopic pictures of skin sections showing normal epidermal and dermal layers with normal skin

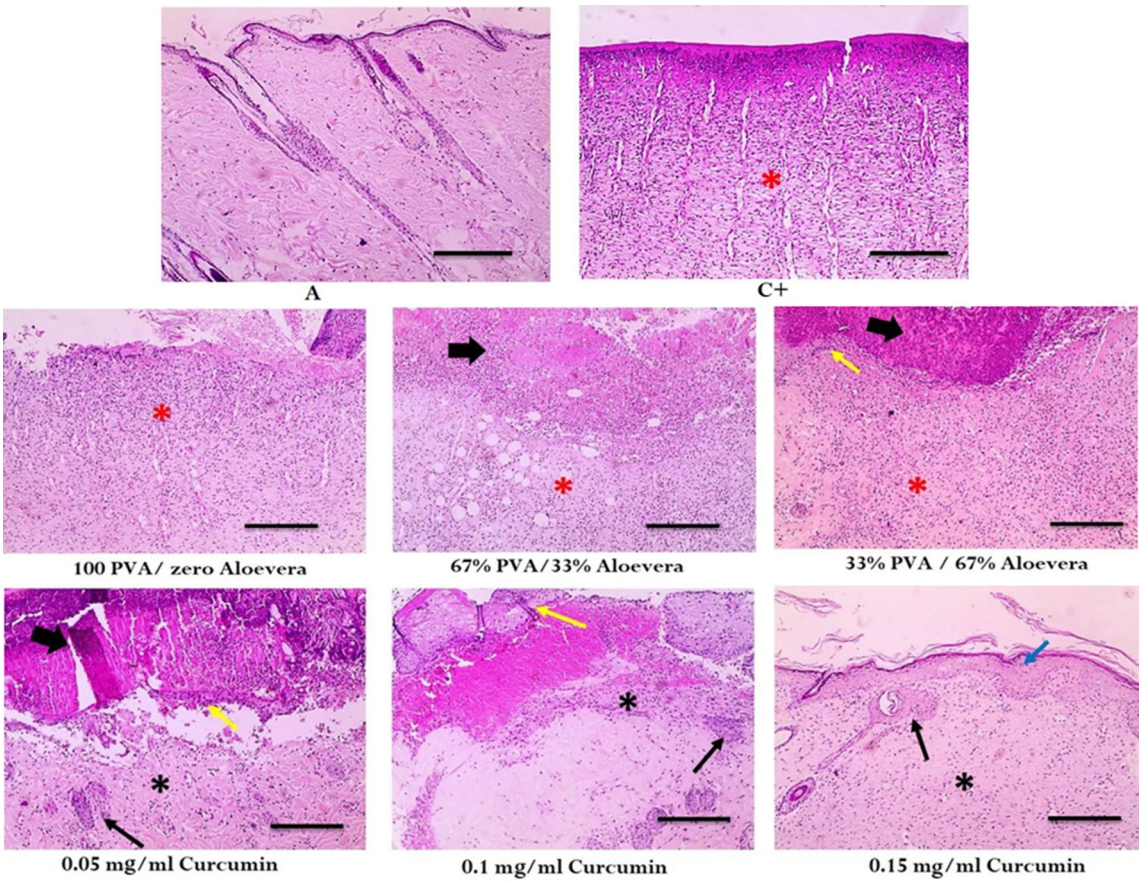

Fig. 10 Representative histological sections of skin tissue for positive and negative control using H&E staining (up) and histological sections of skin tissue regeneration at 14 days' post-treatment for the different groups (middle and down). The sections were stained with H&E staining

appendages in control normal group. Skin sections of control + *Ve* group showing granulation tissue formation filled wound gap (*) infiltrated with poly morphonuclear inflammatory cells (PMNs). Epidermal layer was not formed. *X*: 100.

Figure 10 represents microscopic pictures of skin sections showing wound gap covered with a crusty scab (thick black arrows) in treated groups with 66% PVA/ 34% Aloe vera, 34% PVA/66% Aloe vera and curcumin 0.05 mg/ml. Wound gap is filled with granulation tissue formation (*) in treated groups with 100%PVA/0Aloe vera, 66% PVA/ 34% Aloe vera and 34% PVA/66% Aloe vera. Mature collagen deposition starts (*) in treated groups with 0.05 and 0.1 mg/ml curcumin PVA/Aloe vera membranes. Mature well-organized collagen deposition filled wound gap (*) in treated groups with 0.15 mg/ml curcumin PVA/Aloe vera membranes. New-epithelization (yellow arrows) is seen in treated groups with 34%PVA/66%Aloe vera, 0.05 and 0.1 mg/ml curcumin PVA/Aloe vera films. Full new epidermal layer formation is completed (blue arrows) in treated groups with cur 0.15 mg/ml curcumin PVA/Aloe vera film. Rejuvenation of hair follicles (black arrows) is seen in treated groups with cur 0.5, cur 1 and cur 1.5. *X*: 100.

From Table 6, the histomorphometric results confirmed that the group of Aloe vera treated has slight increase in epitheliogenesis especially for highest Aloe vera content sample in addition to increase in granulation tissue and decrease in inflammation in comparison with control gauze group but noticeable decrease in inflammation with noticeable increase in epitheliogenesis and mature collagen deposition for curcumin-treated groups compared to Aloe vera-treated group and control gauze-treated group; this increase in collagen deposition for curcumin may be due to increase in fibroblasts cells that release *TGF-β* cytokine as reported by Mohanty et al. [22], that confirm the excellent remodeling including the best wound contraction.

4 Conclusions

The PVA/Aloe vera/curcumin hydrogel membranes were developed using short alcohols fully hydrolysing technique for producing physically cross-linking hydrogel membranes.

Table 6 Histomorphometric analysis of all tested groups representing the progress of collagen formation at 14 days' post-treatment

Group	Epitheliogenesis score, Mean ± SE		Granulation tissue, Mean ± SE
Control—ve	0,0,0,0	0.0 ± 0.0 a	0.0 ± 0.0 a
Control + ve	0,0,0,0	0.0 ± 0.0 a	4 ± 0.4 ab
100%PVA/0%Aloe vera	0,0,0,0	0.0 ± 0.0 a	4.5 ± 0.2 ab
66%PVA/34% Aloe vera	0,0,0,0	0.0 ± 0.0 a	4.75 ± 0.0 b
34%PVA/66% Aloe vera	1,0,1,0	0.5 ± 0.2 ab	5 ± 0.0 ab
Curcumin 0.05 mg/ml	1,1,1,0	0.75 ± 0.2 ab	4.5 ± 0.2 ab
Curcumin 0.1 mg/ml	2,2,1,2	1.75 ± 0.2 ab	1.25 ± 0.6 a
Curcumin 0.15 mg/ml	4,4,3,3	3.5 ± 0.2 b	0.0 ± 0.0 ab

Group	Mature collagen deposition, Mean ± SE	Inflammation, Mean ± SE
Control − ve	0.0 ± 0.0 a	0.0 ± 0.0a
Control + ve	0.0 ± 0.0 a	5 ± 0.0 b
100%PVA/0%Aloe vera	0.0 ± 0.0 a	4.5 ± 0.2 b
66%PVA/34% Aloe vera	0.0 ± 0.0 b	3.7 ± 0.25 ab
34%PVA/66% Aloe vera	0.0 ± 0.0 a	2.7 ± 0.4 ab
Curcumin 0.05 mg/ml	3.25 ± 0.2 a	2.2 ± 0.4 ab
Curcumin 0.1 mg/ml	3.7 ± 0.2 a	0.7 ± 0.25 ab
Curcumin 0.15 mg/ml	5 ± 0.0b	0.0 ± 0.0 ab

SE standard error

The PVA/Aloe vera/curcumin films were instrumentally characterized and bioevaluated in vitro and in vivo, as well. FTIR results refer to the absorption peaks that are associated with hydrogen bonds between –OH groups of PVA, verifying the entanglement process. However the addition of Aloe vera and curcumin in physically cross-linked PVA networks influenced significantly their molecular structures and the entire physicochemical properties. SEM results showed alternation in the surface morphology depending on the Aloe vera or curcumin contents in membranes, where surface pores increase with increase in Aloe vera content. Moreover, physically cross-linked PVA/Aloe vera hydrogel exhibited more swollen and elastic membranes, compared to that with only PVA. Aloe vera incorporation to PVA hydrogel improved significantly the thermal stability. Moreover, the overall thermal stability was notably improved by the introduction of Aloe vera as blend materials. Addition of the drug to the film increased the antimicrobial action of Aloe vera and curcumin. From in vitro study, all prepared cross-linked membranes used are safe onto normal cell lines. Further, in vivo assay results showed the moderate effect of Aloe vera in wound healing process. However, the addition of curcumin increased dramatically the healing rate and closure % of the wound; not only increase the healing effect but also by addition of 0.15 mg/mL curcumin makes the wound completely healed by 100% and hair follicles grow in new skin, as illustrated by histological examination. Finally, PVA/Aloe vera/curcumin cross-linked hydrogel membranes are expected as promising biomaterials for improving wound healing of the topical deep and moderated wounds.

Supplementary Information The online version contains supplementary material available at https://doi.org/10.1007/s13369-022-07283-6.

Acknowledgements Authors thank and extend their appreciation to the Scientific Research Fund at Tanta University, Egypt for financing this work through research project code: TU:03-19-02.

Declarations

Conflict of interest The authors declare that they have no conflict of interest.

Ethical statement All experiments were conducted in accordance with the Guidelines of World Medical Association Declaration of Helsinki: Ethical Principles for Medical Research Involving Human Subjects and approved by the ethics committee at Faculty of Science, Tanta University, Egypt.

Open Access This article is licensed under a Creative Commons Attribution 4.0 International License, which permits use, sharing, adaptation, distribution and reproduction in any medium or format, as long as you give appropriate credit to the original author(s) and the source, provide a link to the Creative Commons licence, and indicate if changes were made. The images or other third party material in this article are included in the article's Creative Commons licence, unless indicated otherwise in a credit line to the material. If material is not included in the article's Creative Commons licence and your intended use is not permitted by statutory regulation or exceeds the permitted use, you will need to obtain permission directly from the copyright holder. To view a copy of this licence, visit http://creativecommons.org/licenses/by/4.0/.

References

1. Ullah, F.; Othman, M.B.H.; Javed, F.; Ahmad, Z.; Akil, H.M.: Classification, processing and application of hydrogels: a review. Mater. Sci. Eng., C **57**, 414–433 (2015)
2. Bullock, A.J.; Pickavance, P.; Haddow, D.B.; Rimmer, S.; MacNeil, S.: Development of a calcium-chelating hydrogel for treatment of superficial burns and scalds. Regen. Med. **5**(1), 55–64 (2010)
3. Kamoun, E.A.; Kenawy, E.R.S.; Chen, X.: A review on polymeric hydrogel membranes for wound dressing applications: PVA-based hydrogel dressings. J. Adv. Res. **8**(3), 217–233 (2017)

4. Livolant, F.; Leforestier, A.: Condensed phases of DNA: structures and phase transitions. Prog. Polym. Sci. **21**(6), 1115–1164 (1996)
5. Hollman, P.H.; Katan, M.B.: Dietary flavonoids: intake, health effects and bioavailability. Food Chem. Toxicol. **37**(9–10), 937–942 (1999)
6. Kenawy, E.R.; Abdel-Hay, F.I.; El-Newehy, M.H.; Wnek, G.E.: Controlled release of ketoprofen from electrospun poly (vinyl alcohol) nanofibers. Mater. Sci. Eng. A **459**(1–2), 390–396 (2007)
7. Yang, E.; Qin, X.; Wang, S.: Electrospun crosslinked polyvinyl alcohol membrane. Mater. Lett. **62**(20), 3555–3557 (2008)
8. Kurihara, S.; Sakamaki, S.; Mogi, S.; Ogata, T.; Nonaka, T.: Crosslinking of poly (vinyl alcohol)-graft-*N*-isopropylacrylamide copolymer membranes with glutaraldehyde and permeation of solutes through the membranes. Polymer **37**(7), 1123–1128 (1996)
9. Gao, L.; Seliskar, C.J.: Formulation, characterization, and sensing applications of transparent poly (vinyl alcohol)—polyelectrolyte Blends. Chem. Mater. **10**(9), 2481–2489 (1998)
10. Stauffer, S.R.; Peppast, N.A.: Poly (vinyl alcohol) hydrogels prepared by freezing-thawing cyclic processing. Polymer **33**(18), 3932–3936 (1992)
11. Yao, L.; Haas, T.W.; Guiseppi-Elie, A.; Bowlin, G.L.; Simpson, D.G.; Wnek, G.E.: Electrospinning and stabilization of fully hydrolyzed poly (vinyl alcohol) fibers. Chem. Mater. **15**(9), 1860–1864 (2003)
12. Hamman, J.H.: Composition and applications of Aloe vera leaf gel. Molecules **13**(8), 1599–1616 (2008)
13. Haniadka, R.; Kamble, P.S.; Azmidha, A.; Mane, P.P.; Geevarughese, N.M.; Palatty, P.L.; Baliga, M.S.: Review on the use of Aloe vera (Aloe) in dermatology. In: Bioactive Dietary Factors and Plant Extracts in Dermatology, pp. 125–133. Humana Press, Totowa (2013)
14. Li, X.; Kanjwal, M.A.; Lin, L.; Chronakis, I.S.: Electrospun polyvinyl-alcohol nanofibers as oral fast-dissolving delivery system of caffeine and riboflavin. Colloids Surf. B **103**, 182–188 (2013)
15. Boateng, J.; Catanzano, O.: Advanced therapeutic dressings for effective wound healing—a review. J. Pharm. Sci. **104**(11), 3653–3680 (2015)
16. Hęś, M.; Dziedzic, K.; Górecka, D.; Jędrusek-Golińska, A.; Gujska, E.: Aloe vera (L.) Webb.: natural sources of antioxidants—a review. Plant Foods Hum. Nutr. **74**(3), 255–265 (2019)
17. Stoica, A.E.; Chircov, C.; Grumezescu, A.M.: Hydrogel dressings for the treatment of burn wounds: an up-to-date overview. Materials **13**(12), 2853 (2020)
18. Padhye, S.; Chavan, D.; Pandey, S.; Deshpande, J.; Swamy, K.V.; Sarkar, F.H.: Perspectives on chemopreventive and therapeutic potential of curcumin analogs in medicinal chemistry. Mini-Rev. Med. Chem. **10**(5), 372–387 (2010)
19. Mani, H.; Sidhu, G.S.; Kumari, R.; Gaddipati, J.P.; Seth, P.; Maheshwari, R.K.: Curcumin differentially regulates TGF-β1, its receptors and nitric oxide synthase during impaired wound healing. BioFactors **16**(1, 2), 29–43 (2002)
20. Gopinath, D.; Ahmed, M.R.; Gomathi, K.; Chitra, K.; Sehgal, P.K.; Jayakumar, R.: Dermal wound healing processes with curcumin incorporated collagen films. Biomaterials **25**(10), 1911–1917 (2004)
21. Kulac, M.; Aktas, C.; Tulubas, F.; Uygur, R.; Kanter, M.; Erboga, M.; Ceber, M.; Topcu, B.; Ozen, O.A.: The effects of topical treatment with curcumin on burn wound healing in rats. J. Mol. Histol. **44**(1), 83–90 (2013)
22. Mohanty, C.; Das, M.; Sahoo, S.K.: Sustained wound healing activity of curcumin loaded oleic acid based polymeric bandage in a rat model. Mol. Pharm. **9**(10), 2801–2811 (2012)
23. Thangapazham, R.L.; Sharma, A.; Maheshwari, R.K.: Beneficial role of curcumin in skin diseases. In: The Molecular Targets and Therapeutic Uses of Curcumin in Health and Disease, pp. 343–357 (2007)
24. Aggarwal, B.B.; Harikumar, K.B.: Potential therapeutic effects of curcumin, the anti-inflammatory agent, against neurodegenerative, cardiovascular, pulmonary, metabolic, autoimmune and neoplastic diseases. Int. J. Biochem. Cell Biol. **41**(1), 40–59 (2009)
25. Çakan, D.; Aydın, S.; Demir, G.; Başak, K.: The effect of curcumin on healing in an animal nasal septal perforation model. Laryngoscope **129**(10), E349–E354 (2019)
26. Lim, Z.X.; Cheong, K.Y.: Effects of drying temperature and ethanol concentration on bipolar switching characteristics of natural Aloevera-based memory devices. Phys. Chem. Chem. Phys. **17**(40), 26833–26853 (2015)
27. Jeffrey, G.A.; Saenger, W.: Hydrogen Bonding in Biological Structures. Springer, Berlin (2012)
28. Kenawy, E.R.; Kamoun, E.A.; Eldin, M.S.M.; El-Meligy, M.A.: Physically crosslinked poly (vinyl alcohol)-hydroxyethyl starch blend hydrogel membranes: synthesis and characterization for biomedical applications. Arab. J. Chem. **7**(3), 372–380 (2014)
29. Eldin, M.M.; Hashem, A.I.; Omer, A.M.; Tamer, T.M.: Wound dressing membranes based on chitosan: preparation, characterization and biomedical evaluation. Int. J. Adv. Res. **3**(8), 908–922 (2015)
30. Sharma, B.; Malik, P.; Jain, P.: Biopolymer reinforced nanocomposites: a comprehensive review. Mater. Today Commun. **16**, 353–363 (2018)
31. Trakal, L.; Šigut, R.; Šillerová, H.; Faturíková, D.; Komárek, M.: Copper removal from aqueous solution using biochar: effect of chemical activation. Arab. J. Chem. **7**(1), 43–52 (2014)
32. Dobrovolskaia, M.A.; Clogston, J.D.; Neun, B.W.; Hall, J.B.; Patri, A.K.; McNeil, S.E.: Method for analysis of nanoparticle hemolytic properties in vitro. Nano Lett. **8**(8), 2180–2187 (2008)
33. Chhatri, A.; Bajpai, J.; Bajpai, A.K.; Sandhu, S.S.; Jain, N.; Biswas, J.: Cryogenic fabrication of savlon loaded macroporous blends of alginate and polyvinyl alcohol (PVA). Swelling, de-swelling and antibacterial behaviors. Carbohydr. Polym. **83**(2), 876–882 (2011)
34. Kamble, K.M.; Chimkod, V.B.; Patil, C.S.: Antimicrobial Activity of Aloe Vera Leaf Extract (2013)
35. Valgas, C.; Souza, S.M.D.; Smânia, E.F.; Smania, A., Jr.: Screening methods to determine antibacterial activity of natural products. Braz. J. Microbiol. **38**, 369–380 (2007)
36. Hassan, M.A.; Omer, A.M.; Abbas, E.; Baset, W.M.; Tamer, T.M.: Preparation, physicochemical characterization and antimicrobial activities of novel two phenolic chitosan Schiff base derivatives. Sci. Rep. **8**(1), 1–14 (2018)
37. Mosmann, T.: Rapid colorimetric assay for cellular growth and survival: application to proliferation and cytotoxicity assays. J. Immunol. Methods **65**(1–2), 55–63 (1983)
38. Denizot, F.; Lang, R.: Rapid colorimetric assay for cell growth and survival: modifications to the tetrazolium dye procedure giving improved sensitivity and reliability. J. Immunol. Methods **89**(2), 271–277 (1986)
39. Bahadoran, M.; Shamloo, A.; Nokoorani, Y.D.: Development of a polyvinyl alcohol/sodium alginate hydrogel-based scaffold incorporating bFGF-encapsulated microspheres for accelerated wound healing. Sci. Rep. **10**(1), 1–18 (2020)
40. Sarhan, W.A.; Azzazy, H.M.; El-Sherbiny, I.M.: Honey/chitosan nanofiber wound dressing enriched with Allium sativum and Cleome droserifolia: enhanced antimicrobial and wound healing activity. ACS Appl. Mater. Interfaces **8**(10), 6379–6390 (2016)
41. Book, Klein and Goldberg.pdf: Open Education Resource (OER) Libre Texts Project, California state university learning program, USA. In: Chapter13: Alcohols and Phenols, Physical Properties of Alcohols: Hydrogen Bonding. 17/9/2021 (n.d.)
42. Farid, E.; Kamoun, E.A.; Taha, T.H.; El-Dessouky, A.; Khalil, T.E.: PVA/CMC/attapulgite clay composite hydrogel membranes

for biomedical applications: factors affecting hydrogel membranes crosslinking and bio-evaluation tests. J. Polym. Environ. **22**, 2538–2545 (2022)
43. Kenawy, E.S.; Kamoun, E.A.; Serag Eldin, M.; Soliman, H.M.A.; El-Moslamy, S.H.; El-Fakharany, E.M.; Shokr, A.M.: Electrospun PVA–dextran nanofibrous scaffolds for acceleration of topical wound healing: nanofiber optimization, characterization and in vitro assessment. Arab. J. Sci. Eng. 1–18 (2022)
44. Bonilla, J.; Fortunati, E.L.E.N.A.; Atarés, L.; Chiralt, A.; Kenny, J.M.: Physical, structural and antimicrobial properties of poly vinyl alcohol–chitosan biodegradable films. Food Hydrocolloids **35**, 463–470 (2014)
45. El Miri, N.; Abdelouahdi, K.; Zahouily, M.; Fihri, A.; Barakat, A.; Solhy, A.; El Achaby, M.: Bio-nanocomposite films based on cellulose nanocrystals filled polyvinyl alcohol/chitosan polymer blend. J. Appl. Polym. Sci. 132(22) (2015)
46. Kolev, T.M.; Velcheva, E.A.; Stamboliyska, B.A.; Spiteller, M.: DFT and experimental studies of the structure and vibrational spectra of curcumin. Int. J. Quantum Chem. **102**(6), 1069–1079 (2005)
47. Mansur, H.S.; Oréfice, R.L.; Mansur, A.A.: Characterization of poly (vinyl alcohol)/poly (ethylene glycol) hydrogels and PVA-derived hybrids by small-angle X-ray scattering and FTIR spectroscopy. Polymer **45**(21), 7193–7202 (2004)
48. Feiz, S.; Navarchian, A.H.; Jazani, O.M.: Poly (vinyl alcohol) membranes in wound-dressing application: microstructure, physical properties, and drug release behavior. Iran. Polym. J. **27**(3), 193–205 (2018)
49. Shiraishi, M.; Inagaki, M.: X-ray diffraction methods to study crystallite size and lattice constants of carbon materials. In: Carbon Alloys, pp. 161–173. Elsevier, Amsterdam (2003)
50. Kamoun, E.A.; Loutfy, S.A.; Hussien, Y.; Kenawy, E.S.: Recent advances in PVA-polysaccharide based hydrogels and electrospun nanofibers in biomedical applications: a review. Int J Biol Macrmol **187**, 755–768 (2021)
51. El-Lakany, S.A.; Abd-Elhamid, A.I.; Kamoun, E.A.; El-Fakharany, E.M.; Samy, W.M.; Elgindy, N.A.: α-Bisabolol-loaded cross-linked zein nanofibrous 3D-scaffolds for accelerating wound healing and tissue regeneration in rats. Int J Nanomed **4**, 8251–8270 (2019)
52. Yetim, I.; Özkan, O.V.; Dervişoglu, A.; Erzurumlu, K.; Canbolant, E.: Effect of local gentamicin application on healing and wound infection in patients with modified radical mastectomy: a prospective randomized study. J. Int. Med. Res. **38**(4), 1442–1447 (2010)
53. Holzer, B.; Grüssner, U.; Brückner, B.; Houf, M.; Kiffner, E.; Schildberg, F.W.; EMD Study Group: Efficacy and tolerance of a new gentamicin collagen fleece (Septocoll®) after surgical treatment of a pilonidal sinus. Colorectal Dis. 5(3), 222–227 (2003)
54. Eklund, A.M.: Prevention of sternal wound infections with locally administered gentamicin. APMIS **115**(9), 1022–1024 (2007)
55. Picó, R.B.; Jiménez, L.A.; Sánchez, M.C.; Castelló, C.H.; Bilbao, A.M.; Arias, M.P.; Ramirez, R.V.: Prospective study comparing the incidence of wound infection following appendectomy for acute appendicitis in children: conventional treatment versus using reabsorbable antibacterial suture or gentamicin-impregnated collagen fleeces. Cir. Pediátr. Organo Oficial Soc. Esp. Cir. Pediátr. **21**(4), 199–202 (2008)
56. Cavanaugh, D.L.; Berry, J.; Yarboro, S.R.; Dahners, L.E.: Better prophylaxis against surgical site infection with local as well as systemic antibiotics: an in vivo study. J. Bone Joint Surg. **91**(8), 1907 (2009)
57. Rutten, H.J.; Nijhuis, P.H.: Prevention of wound infection in elective colorectal surgery by local application of a gentamicin-containing collagen sponge. Eur. J. Surg. Supplem. Acta Chir. Supplem. **578**, 31–35 (1997)
58. Hussien, Y.; Loutfy, S.A.; Kamoun, E.A.; El-Mosalmy, S.H.; Radwan, E.M.; Elbehairi, S.E.I.: Enhanced anti-cancer activity by localized delivery of curcumin form PVA/CNCs hydrogel membranes: preparation and in vitro bioevaluation. Int. J. Biol. Macromol. **170**, 107–122 (2021)
59. Pucino, N.; Kennedy, D.M.; Carvalho, R.C.; Allan, B.; Ierodiaconou, D.: Citizen science for monitoring seasonal-scale beach erosion and behaviour with aerial drones. Sci. Rep. **11**(1), 1–17 (2021)
60. Kenawy, E.; Omer, A.M.; Tamer, T.M.; Elmeligy, M.A.; Eldin, M.M.: Fabrication of biodegradable gelatin/chitosan/cinnamaldehyde crosslinked membranes for antibacterial wound dressing applications. Int. J. Biol. Macromol. **139**, 440–448 (2019)
61. Tamer, T.M.; Valachová, K.; Hassan, M.A.; Omer, A.M.; El-Shafeey, M.; Eldin, M.S.M.; Šoltés, L.: Chitosan/hyaluronan/edaravone membranes for anti-inflammatory wound dressing: In vitro and in vivo evaluation studies. Mater. Sci. Eng. C **90**, 227–235 (2018)
62. Grindlay, D.; Reynolds, T.: The Aloe vera phenomenon: a review of the properties and modern uses of the leaf parenchyma gel. J. Ethnopharmacol. **16**(2–3), 117–151 (1986)
63. Takzare, N.; Hosseini, M.J.; Hasanzadeh, G.; Mortazavi, H.; Takzare, A.; Habibi, P.: Influence of Aloe Vera gel on dermal wound healing process in rat. Toxicol. Mech. Methods **19**(1), 73–77 (2009)
64. Chithra, P.; Sajithlal, G.B.; Chandrakasan, G.: Influence of Aloe vera on the healing of dermal wounds in diabetic rats. J. Ethnopharmacol. **59**(3), 195–201 (1998)
65. Sasaki, T.: The effects of basic fibroblast growth factor and doxorubicin on cultured human skin fibroblasts: relevance to wound healing. J. Dermatol. **19**(11), 664–666 (1992)
66. Werner, S.: A novel enhancer of the wound healing process: the fibroblast growth factor-binding protein. Am. J. Pathol. **179**(5), 2144 (2011)
67. Akbik, D.; Ghadiri, M.; Chrzanowski, W.; Rohanizadeh, R.: Curcumin as a wound healing agent. Life Sci. **116**(1), 1–7 (2014)
68. Emiroglu, G.; Ozergin Coskun, Z.; Kalkan, Y.; Celebi Erdivanli, O.; Tumkaya, L.; Terzi, S.; Dursun, E.: The effects of curcumin on wound healing in a rat model of nasal mucosal trauma. Evid.-Based Complem. Altern. Med. 2017 (2017)